Quaternary Structure of Carbonmonoxyhemoglobins in Solution: Structural Changes Induced by the Allosteric Effector Inositol Hexaphosphate†

Qingguo Gong,‡ Virgil Simplaceanu,‡ Jonathan A. Lukin,§ Janel L. Giovannelli,‡ Nancy T. Ho,‡ and Chien Ho*,‡

Department of Biological Sciences, Carnegie Mellon University, Pittsburgh, Pennsylvania 15213, and Clinical Genomics Centre, University Health Network, Toronto, Ontario, Canada

Received November 28, 2005; Revised Manuscript Received February 14, 2006

ABSTRACT: We have applied the residual dipolar coupling (RDC) method to investigate the solution quaternary structures of ^{2}H- and ^{15}N-labeled human normal adult recombinant hemoglobin (rHb A) and a low-oxygen-affinity mutant recombinant hemoglobin, rHb(α96Val→Trp), both in the carbonmonoxy form, in the absence and presence of an allosteric effector, inositol hexaphosphate (IHP), using a stretched polyacrylamide gel as the alignment medium. Our recent RDC results [Lukin, J. A., Kontaxis, G., Simplaceanu, V., Yuan, Y., Bax, A., and Ho, C. (2003) *Proc. Natl. Acad. Sci. U.S.A. 100*, 517−520] indicate that the quaternary structure of HbCO A in solution is a dynamic ensemble between two previously determined crystal structures, R (crystals grown under high-salt conditions) and R2 (crystals grown under low-salt conditions). On the basis of a comparison of the geometric coordinates of the T, R, and R2 structures, it has been suggested that the oxygenation of Hb A follows the transition pathway from T to R and then to R2, with R being the intermediate structure [Srinivasan, R., and Rose, G. D. (1994) *Proc. Natl. Acad. Sci. U.S.A. 91*, 11113−11117]. The results presented here suggest that IHP can shift the solution quaternary structure of HbCO A slightly toward the R structure. The solution quaternary structure of rHbCO(α96Val→Trp) in the absence of IHP is similar to that of HbCO A in the presence of IHP, consistent with rHbCO(α96Val→Trp) having an affinity for oxygen lower than that of Hb A. Moreover, IHP has a much stronger effect in shifting the solution quaternary structure of rHbCO(α96Val→Trp) toward the R structure and toward the T structure, consistent with IHP causing a more pronounced decrease in its oxygen affinity. The results presented in this work, as well as other results recently reported in the literature, clearly indicate that there are multiple quaternary structures for the ligated form of hemoglobin. These results also provide new insights regarding the roles of allosteric effectors in regulating the structure and function of hemoglobin. The classical two-state/two-structure allosteric mechanism for the cooperative oxygenation of hemoglobin cannot account for the structural and functional properties of this protein and needs to be revised.

Human normal adult hemoglobin (Hb A)[1] has four subunits, i.e., two α-chains of 141 amino acid residues each and two β-chains of 146 amino acid residues each (*1*). The classical X-ray crystallographic structural analyses indicated that there are two distinct quaternary structures, namely, the deoxy or unligated state, represented by the tense (T), low-affinity structure, and the ligated state, represented by the relaxed (R), high-affinity structure (*2*). Both types of crystal structure were obtained from crystals grown under high-salt conditions (*3*). Several quaternary structures of ligated hemoglobin, in particular in the carbonmonoxy form, have been observed more recently, when crystals are grown under high- or low-salt conditions. Arnone and co-workers (*4*) reported a new R structure, known as the R2 structure, when HbCO crystals were grown under low-salt and -pH conditions. More recently, Safo et al. (*5*) reported that the R2 structure can also be crystallized under high-salt conditions. The difference between the R and R2 structures is found to be comparable in magnitude to that between the T and R structures. Mueser et al. (*6*) reported that the R structure for bovine HbCO is not unique but depends on the crystallization conditions. By a comparison of the geometric coordinates of the T, R, and R2 structures, Srinivasan and Rose (*7*) concluded that in going from the deoxy to the ligated form, the quaternary structure goes from T to R and then to R2; i.e., R is the intermediate state. More recently, two additional X-ray quaternary structures termed R3 and RR2 have been found in the family of ligated Hb A structures by Safo and Abraham (*8*). They found that the R3 structure is an end

† This work is supported by research grants from the National Institutes of Health (R01HL-024525 and S10RR-017815).

* To whom correspondence should be addressed: Department of Biological Sciences, Carnegie Mellon University, 4400 Fifth Ave., Pittsburgh, PA 15213. Telephone: (412) 268-3395. Fax: (412) 268-7083. E-mail: chienho@andrew.cmu.edu.

‡ Carnegie Mellon University.

§ University Health Network.

[1] Abbreviations: Hb A, human normal adult hemoglobin; HbCO, carbonmonoxyhemoglobin; rHb, recombinant hemoglobin; NMR, nuclear magnetic resonance; RDC, residual dipolar coupling; 2,3-BPG, 2,3-bisphosphoglycerate; IHP, inositol hexaphosphate; BZF, benzafibrate; TEMED, *N*,*N*,*N*′,*N*′-tetramethylethylenediamine; HSQC, heteronuclear single-quantum coherence; TROSY, transverse relaxation-optimized spectroscopy; SVD, singular-value decomposition; rmsd, root-mean-square deviation; D_a, alignment tensor; P_{50}, partial pressure of oxygen at 50% saturation; n_{50}, Hill coefficient at 50% oxygen saturation.

10.1021/bi052424h CCC: $33.50
Published on Web 04/01/2006

state and exhibits a quaternary structure difference from the T structure as large as that of the R2 structure from the T structure, but in a different direction, as defined by a rigid-body screw rotation, while the RR2 structure is described as an intermediate conformation between the R and R2 structures. By measuring $^{15}N-^{1}H$ residual dipolar couplings (RDCs) of HbCO A in two different aqueous liquid crystalline media, phospholipid bicelles and filamentous bacteriophage Pf1, we have found that the quaternary conformation of HbCO A in solution is a dynamic ensemble of the two previously determined crystal structures R (crystals grown under high-salt conditions) and R2 (crystals grown under low-salt conditions) (*9*).

It is known that allosteric effectors, such as hydrogen ions, chloride ions, and organic phosphates, e.g., 2,3-bisphosphoglycerate (2,3-BPG) and inositol hexaphosphate (IHP), modulate the oxygen affinity of hemoglobin (*1*). The effect of 2,3-BPG and IHP (in particular the latter) on the oxygen affinity of Hb A is pronounced. Arnone (*10*) reported that 2,3-BPG binds to the central cavity of the Hb molecule in the deoxy form, specifically to βVal1, βHis2, βLys82, and βHis143, and thus stabilizes the deoxy quaternary form and lowers the oxygen affinity. Arnone and Perutz (*11*) reported that IHP also binds to the central cavity of the deoxy-Hb A molecule, specifically at amino residues βHis2, βLys82, βAsp139, and βHis143. There are no structural data on HbCO A in the presence of IHP. According to Arnone and co-workers (*12*), IHP is very disordered in the low-salt quaternary T crystals, and therefore, they have not modeled the IHP molecule in its $\beta-\beta$ binding site. Recently, Yonetani et al. (*13*) reported that allosteric effectors, such as 2,3-BPG, benzafibrate (BZF), and IHP, affect only ligation-linked tertiary structural changes rather than the homotropic ligation-linked T−R quaternary structural transition. It thus appears that the role of allosteric effectors in the structure−function relationship of Hb A is not fully understood. Indeed, this is an important question not only for hemoglobin but also for the field of allostery in general.

A number of studies have been reported in the literature regarding structural and functional changes induced by IHP in Hb A and mutant Hbs (*11*, *13*−*18*). A common assumption made in a two-structure allosteric model is that the presence of allosteric effectors shifts the equilibrium to the T quaternary structure, thus lowering the oxygen affinity of Hb. There is so far no definitive evidence that the binding of IHP to Hb A can produce a new quaternary structure of Hb A in solution, i.e., different from the classical T and R structures. In the work presented here, we have extended the use of RDC measurements (*9*) to determine the solution structure of HbCO A using a different alignment medium and to investigate the quaternary structure of HbCO A in the presence of IHP. To confirm our hypothesis that IHP induces a quaternary structural shift from R2 toward R in HbCO A, we have also investigated the solution structure of a low-oxygen-affinity mutant Hb, rHb(α96Val→Trp), with and without IHP. We have found previously (*15*) that this rHb exhibits low oxygen affinity and high cooperativity and can switch its structure from R- to T-like at 10 °C upon addition of IHP, while remaining ligated with CO. The crystal structures for this rHb in both the ligated and unligated states have also been determined (*19*).

MATERIALS AND METHODS

Preparation of ^{2}H- and ^{15}N-Labeled rHb Samples. Chain-specific ^{2}H- and ^{15}N-labeled rHbCO samples, namely, ^{2}H- and ^{15}N-labeled α-chain combined with unlabeled normal β-chain and unlabeled α-chain combined with ^{2}H- and ^{15}N-labeled β-chain, were prepared as described by Simplaceanu et al. (*20*). rHb(α96Val→Trp) was expressed using pHE202 in *Escherichia coli* JM109 (*15*). The chain-specific ^{2}H- and ^{15}N-labeled-rHbCO(α96Val→Trp) samples (i.e., ^{2}H- and ^{15}N-labeled mutated α-chain combined with unlabeled normal β-chain and unlabeled mutated α-chain combined with ^{2}H- and ^{15}N-labeled normal β-chain) were prepared in a manner similar to that for the rHbCO A samples.

Alignment Medium Using a Stretched Polyacrylamide Gel. One milliliter of a 3.75% polyacrylamide gel was prepared by mixing 125 μL of 30% acrylamide (1:37.5 bisacrylamide by weight), 865 μL of H_2O, 10 μL of 10% ammonium persulfate, and 0.8 μL of *N*,*N*,*N*′,*N*′-tetramethylethylenediamine (TEMED). Immediately after mixing, 400 μL of the solution was pipetted into a Teflon gel chamber (6 mm inside diameter, New Era, Vineland, NJ) sealed at one end with Parafilm, and 45−60 min allowed for polymerization. The gel was then gently transferred to distilled water and washed for 2−3 days. Then, it was allowed to dry in air until most of the water had evaporated and the gel had shrunk in size. The gel was then carefully moved back to the Teflon gel chamber. An excess amount of 450 μL of a concentrated HbCO A solution was added to the gel at the bottom of the Teflon chamber. The top end was sealed with Parafilm, and the chamber was incubated vertically in a sealed container filled with CO gas at 30 °C for 7 days to allow the gel to be completely rehydrated and the hemoglobin to diffuse evenly. The gel was then loaded carefully into an open-ended NMR tube (4.2 mm inside diameter) directly from the chamber using a funnel-like mechanical apparatus (New Era). An end plug with an O-ring was used to seal the bottom of the open-ended tube, while the top end was closed with a Shigemi (Allison Park, PA) microcell plunger. At all times, the sample was carefully kept under a CO gas atmosphere to prevent contamination with oxygen.

As an alignment medium, a stretched polyacrylamide gel at a fixed concentration yields a 2-fold stronger alignment when compressed radially than when compressed axially (*21*). Therefore, radial compression permits the use of lower gel concentrations, allowing for more protein in the sample. A gel with a concentration below 3% is too dilute to maintain enough mechanical strength for transfer between the gel chamber and the NMR tube. We have found that a gel concentration of 3−4% is the best choice for our Hb samples among the concentrations that we have tested (3−8%). The higher gel concentrations resulted in excessive line broadening and spectral distortions of the NMR spectra.

NMR Experiments and Data Processing. Samples in gel were prepared from Hb solutions of typically 1.5−2.0 mM (tetramer), chain-specifically labeled (^{2}H,^{15}N)rHbCO A, prepared as previously described in 0.1 M sodium phosphate buffer at pH 7.0 and in 90% H_2O and 10% D_2O. The actual concentration in the gel varied slightly. The samples for the isotropic spectra were typically 1 mM in tetramer. All spectra were collected at 35 °C on a Bruker DRX-600 NMR

Table 1: Fitted Parameters for HbCO A and rHbCO(αV96W) in the Presence and Absence of IHP

	IHP	x^a	x_{error}	$D_a{}^b$ (Hz)	ϕ^c	$R_h{}^d$	$\chi_v{}^{2\,e}$	rmsd^f (Hz)
HbCO A	−	0.52	0.12	−11.13	88.92	0.016	53.56	1.23
HbCO A	+	0.45	0.13	−11.62	89.39	0.079	33.79	1.41
rHbCO(αV96W)	−	0.46	0.13	−12.53	89.50	0.013	20.73	1.61
rHbCO(αV96W)	+	0.20	0.14	−12.14	90.91	0.033	13.46	1.58

[a] Quaternary coordinate corresponding to the optimal conformation. [b] Magnitude of the alignment tensor. [c] Angle between the principal *z*-axis of the alignment tensor and the R ↔ R2 dimer rotation axis. [d] Rhombicity of the alignment tensor. [e] χ^2 corresponding to the optimal conformation. [f] Root-mean-square deviation between observed RDCs and calculated RDCs.

Table 2: Oxygen Binding Properties of Hb A and rHb(αV96W) (0.1 mM each) in 0.1 M Sodium Phosphate at pH 7.0 and 35 °C with and without 0.3 mM IHP

	[IHP] (mM)	P_{50} (mmHg)	n_{50}
Hb A	0	18.9	2.9
Hb A	0.3	40.0	2.4
rHb(αV96W)	0	29.6	2.5
rHb(αV96W)	0.3	54.5	2.0

spectrometer operating at 14.1 T. Interleaved heteronuclear single-quantum coherence (HSQC) and temperature-compensated transverse relaxation-optimized spectroscopy (TROSY) measurements in the presence and absence of aligning medium, with and without 3 mM IHP, were collected to measure the one-bond $^{15}N-^{1}H$ splitting ($^1J_{NH} + {}^1D_{NH}$). The RDCs of the peaks, which were previously assigned (*22*), were reasonably well resolved in the HSQC spectra, and correspond to amino acid residues located in the α-helical regions of the protein, have been chosen to fit the following equation (*23*):

$$^1D_{NH} = D_a[(3\cos^2\theta - 1) + {}^3/_2 R_h \sin^2\theta \cos 2\varphi] \quad (1)$$

where D_a and R_h are the magnitude and rhombicity of the alignment tensor, respectively, and the polar angles θ and φ describe the orientation of the NH bond vector with respect to the alignment frame. Fits were performed by using singular-value decomposition (SVD) or nonlinear least-squares methods. The uncertainties for the best-fit quaternary structures were estimated by using fitted parameters under various experimental conditions (Table 1), as described previously (*9*).

Oxygen Binding Properties of Hb A and rHb(α96Val→Trp). For the Hb A and rHb(α96Val→Trp) [also called rHbCO(αV96W)] samples (0.1 mM for each), with and without IHP, oxygen dissociation curves were measured by a Hemox-Analyzer (TCS Medical Products, Huntington Valley, PA) at 35 °C in 0.1 M sodium phosphate buffer at pH 7.0. Catalase and superoxide dismutase (Sigma) were added (final concentrations of 0.3 μM) to prevent the formation of methemoglobin. The partial O_2 pressure at 50% saturation (P_{50}) (a measure of oxygen affinity) and the Hill coefficient (n_{50}) at 50% oxygen saturation (a measure of the cooperativity in the oxygenation process) were determined from each curve (Table 2). The accuracy for the P_{50} measurements is ±5%, and that for n_{50} is ±10%.

RESULTS

Alignment of HbCO A Using a Stretched Polyacrylamide Gel. For HbCO A, the magnitude of the alignment tensor (D_a) fitted for the optimal quaternary structure in a 3.75% polyacrylamide gel is −11.13 Hz (Table 1), which is in perfect agreement with the value of −11.36 Hz measured in bicelles (*9*). The angle (ϕ) between the principal *z*-axis of the alignment tensor and the R−R2 dimer rotation axis measured in gel and bicelles is also similar, 89° and 82°, respectively. These results indicate that these two alignment media provide a similar alignment frame and the same degree of alignment.

NMR Investigations of HbCO A and rHbCO(αV96W). In comparing the HSQC spectra of the α- and β-chains of chain-specific ^2H- and ^{15}N-labeled rHbCO A samples, we have observed little significant signal loss or spectral rearrangement upon the binding of IHP, indicating that HbCO A largely preserves its normal conformation in the presence of IHP. However, several amino acid residues within the regions of residues 2−9, 39−42, 78−81, 85−97, and 135−137 in the α-chain as well as Leu3, Lys82, Gly83, and residues 99−101 and 138−146 in the β-chain clearly undergo small chemical shift changes (Figure 1A). By carefully tracking these changes in the chemical shifts, we are able to assign the backbone resonances of the complex between HbCO A and IHP and investigate the quaternary structural changes of HbCO A in the presence of IHP. For rHbCO(αV96W), most of the peaks in the HSQC spectra of the α- and β-chains at 35 °C can be superimposed very well on the corresponding peaks of HbCO A, suggesting that rHbCO(αV96W) possesses an overall structure very similar to that of Hb A, in agreement with our previous one-dimensional ^1H NMR spectra and X-ray crystal structures of this rHb (*15*, *19*). However, several peaks in the HSQC spectra of rHbCO(αV96W) exhibit large chemical shift changes due to structural changes resulting from the amino acid substitution at position α96, as shown in the one-dimensional ^1H NMR spectra and in the crystal structure. These peaks belong to residues located at the $\alpha_1\beta_2$ interface, such as αLeu100, βGlu101, and βArg104 (Figure 1B). It has been reported in a previous X-ray crystal structure investigation that in the R state of this mutant rHb, the newly introduced αTrp96 contacts several of its neighboring amino acid residues, i.e., αLys99, βAsp99, and βGlu101, either through van der Waals or through oxygen−aromatic interactions, and thus alters the conformations of these residues in rHbCO(αV96W) compared to the corresponding residues in HbCO A (*19*). The shifted resonances that we have observed are consistent with the residues in direct or indirect contact with αTrp96. Upon the addition of IHP, additional peak shifts as well as intensity changes have been observed in the HSQC spectra of rHbCO(αV96W) in comparison with the spectra of HbCO A (Figure 1C). Several peaks become much broader in the presence of IHP, implying the existence of multiple conformations for those amino acid residues. Backbone resonances assigned to αThr39, αThr41, αTyr42, αHis89, αLys90, αArg92, αTrp96, and αLeu100 either become weak or lose most of their intensity. The significant signal intensity loss for residues β90−97 and β140−146, and the disappearance of the resonances of βTrp37, βThr38, βGlu101, βAsn102, and βArg104, indicate larger local conformational

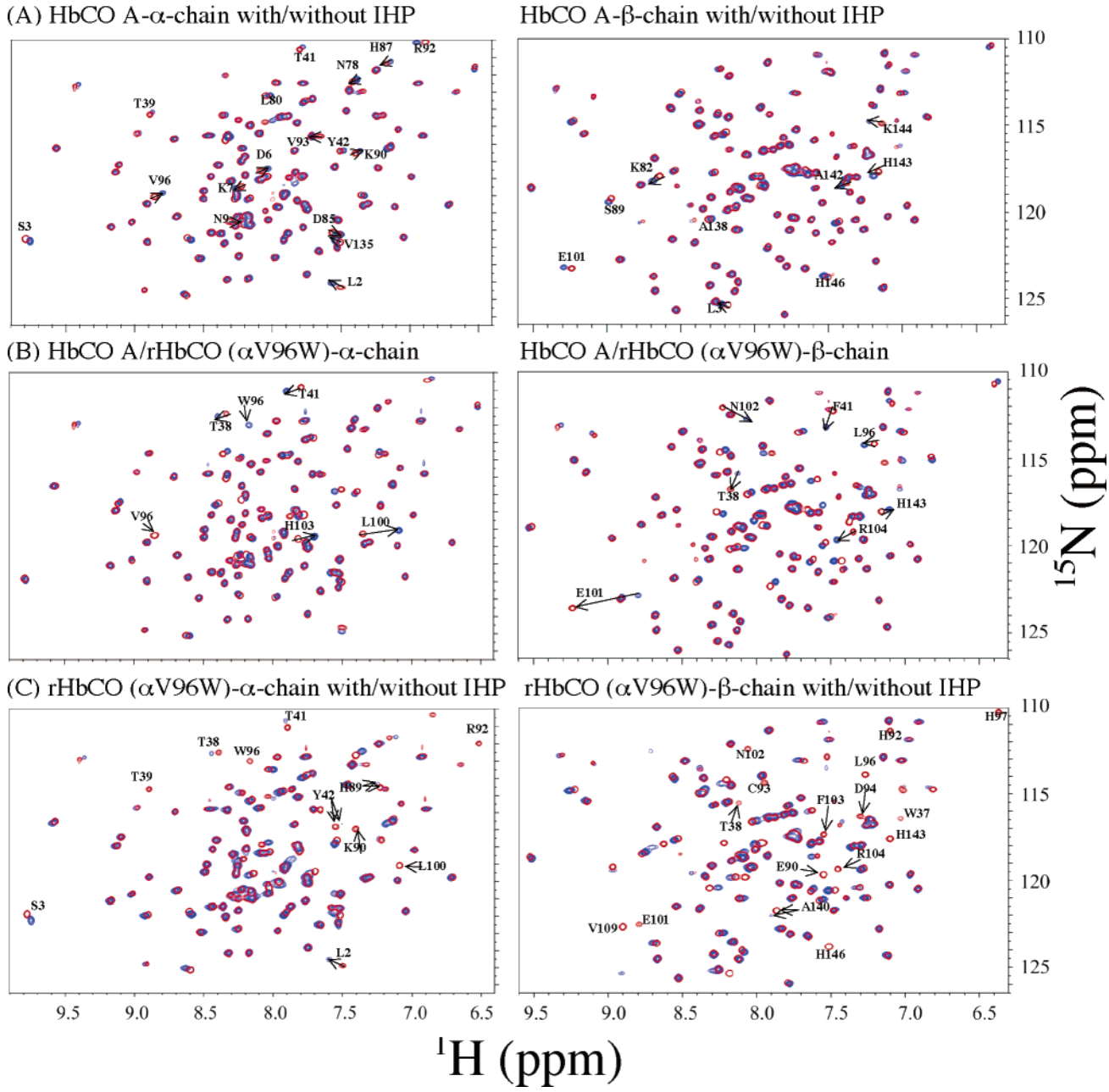

FIGURE 1: (A) Superposition of HSQC spectra of the HbCO A α-chain (left) and *β*-chain (right) in the absence (red) and presence (blue) of IHP at 35 °C. Some resonances that have an obvious chemical shift change are labeled. (B) Superposition of HSQC spectra of the α-chain (left) and *β*-chain (right) of HbCO A (red) and rHbCO(αV96W) (blue) at 35 °C. Some resonances that exhibit large chemical shift changes are labeled. (C) Superposition of HSQC spectra of the rHbCO(αV96W) α-chain (left) and *β*-chain (right) in the absence (red) and presence (blue) of IHP at 35 °C. The resonances that either disappear or significantly lose intensity are labeled.

and dynamical changes upon IHP binding in the *β*-chain than in the α-chain of this rHb.

Effects of IHP on the Structures of HbCO A and rHbCO-(αV96W). Using the coordinates for the α*β* dimer subunits derived from the accurate R2 (PDB entry 1BBB) crystal structure of HbCO A, the RDCs measured in a 3.75% polyacrylamide gel have been used to fit a series of intermediate quaternary structures generated by reorienting the $\alpha_2\beta_2$ dimer stepwise relative to the $\alpha_1\beta_1$ dimer along the pathway of the R2 → R structure transformation as described by Lukin et al. (*9*). By fitting the $^{15}N-^{1}H$ RDCs obtained by using the HSQC-TROSY method to investigate the structures from R2 to R, we have obtained a parabolic curve (reduced χ^2 plotted against the quaternary coordinate *x*) with a minimum at $x = 0.52 \pm 0.12$ (Figure 2A), where $x = 0$ forthe R state and $x = 1$ for the R2 state. This result is in perfect agreement with our previous results using bicelles and phage Pf1 as the alignment media, which show that the actual solution structure of HbCO A is a dynamic intermediate, approximately halfway between the R and R2 conformations ($x = 0.51 \pm 0.13$ in bicelles) (*9*). Upon addition of the allosteric effector, IHP, the minimum of the fitted curve shifts toward the R structure, i.e., from 0.52 ± 0.12 to 0.45 ± 0.13. The difference between the corresponding best-fit structures in terms of *x* is only −0.07.

We have found from our RDC measurements that in the absence of IHP, rHbCO(αV96W) exhibits a quaternary coordinate of 0.46 ± 0.13 (Figure 2C), a value very similar to that for HbCO A in the presence of IHP ($x = 0.45 \pm 0.13$). Upon addition of IHP to rHb(αV96W), the optimal

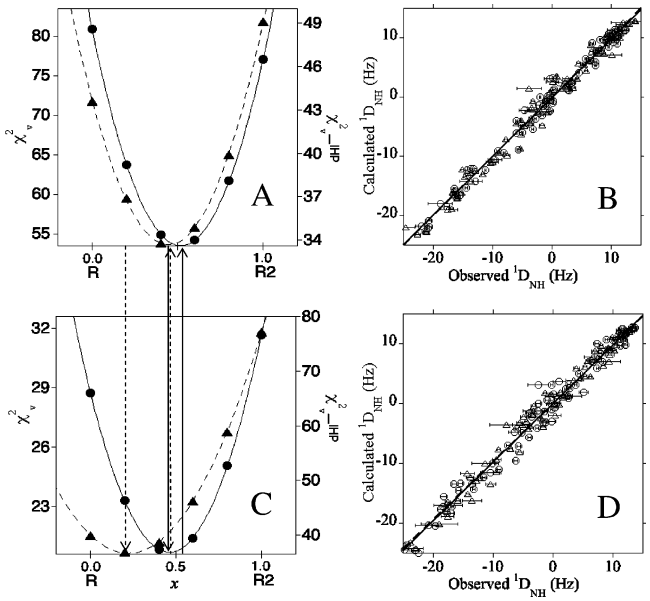

FIGURE 2: Comparison of reduced χ^2 values of best fits of RDCs vs quaternary coordinate x from R to R2 for HbCO A (A) and rHbCO(αV96W) (C) at pH 7.0 and 35 °C. The dashed lines and solid lines are used to highlight the optimum on the parabolic curves in the presence (▲) and absence (●) of IHP, respectively. The corresponding optimal structure shifts from 0.52 ± 0.12 to 0.45 ± 0.13 in HbCO A upon addition of IHP. A larger shift from 0.46 ± 0.13 to 0.20 ± 0.14 is observed in rHbCO(αV96W). Calculated vs observed RDCs for the best fit of the corresponding optimal structure in the presence (△) and absence (○) of IHP are plotted for HbCO A and rHbCO(αV96W) in panels B and D. Errors for the observed RDCs, calculated as described by Bax et al. (*44*), are shown as horizontal error bars. The rmsds of the best fits with and without IHP are 1.41 and 1.23 Hz for HbCO A and 1.58 and 1.61 Hz for rHbCO(αV96W), respectively.

quaternary coordinate is shifted dramatically to 0.20 ± 0.14, showing an IHP effect of −0.26. This finding clearly demonstrates that rHb(αV96W) exhibits a new quaternary structure in solution that is displaced away from the R2 and toward the R structure.

Effect of IHP on the Oxygen Affinity of Hb A and rHb(αV96W). Oxygen binding properties of Hb A and rHb(αV96W) measured under the same conditions used for the NMR experiments are summarized in Table 2. In 0.1 M sodium phosphate buffer at pH 7.0 and 35 °C, rHb(αV96W) exhibits a larger IHP-induced oxygen affinity reduction than Hb A according to the change in P_{50}. Both Hb A and rHb(αV96W) exhibit similar cooperativity changes with n_{50} values (a measure of cooperativity of the oxygenation process) altered from 2.9 to 2.4 and from 2.5 to 2.0 in the absence and presence of IHP, respectively.

DISCUSSION

Functional Role of Quaternary Structure Change in Hemoglobin. An important but unresolved issue in hemoglobin research is the precise role of allosteric effectors in regulating the structure and function of the protein molecule. A two-structure allosteric model would suggest that an allosteric effector would shift the T−R equilibrium toward the T structure, thus reducing the ligand affinity as suggested by the stereochemical mechanism for the cooperative oxygenation of Hb first postulated by Perutz (*2*). Another interpretation of the role of an allosteric effector is that it merely alters the tertiary structure of the Hb molecule, thus altering the ligand affinity. This point of view is advocated by Yonetani et al. (*13*). Another possible interpretation is that an allosteric effector can alter both quaternary and tertiary structures of the Hb molecule, thus altering its ligand affinity. To support the third alternative, we need to find out if a new quaternary structure differing from the classical T and R structures exists in solution and whether this new quaternary structure can correlate with the altered ligand affinity upon addition of an allosteric effector to the Hb molecule.

Table 3: Comparison of Fitted Parameters and rmsds between Measured and Calculated RDCs for the Best-Fit Quaternary Structure of the Low-Affinity Mutant rHb(αV96W) Based on the High-Resolution 1BBB (Hb A) and 1RVW (αV96W) PDB Crystal Structures for the $\alpha\beta$ Dimer Subunits in the Absence and Presence of IHP

PDB entry	IHP	D_a (Hz)	R_h	rmsd (Hz)
1BBB	−	−12.33	0.004	1.785
1BBB	+	−12.04	0.022	1.643
1RVW	−	−11.81	0.010	2.727
1RVW	+	−11.07	0.005	3.179

In this study, we have applied the RDC method to investigate the solution structures of HbCO A and rHbCO(αV96W) in the absence and presence of a powerful allosteric effector, IHP. Our NMR results clearly show that there are obvious local conformational changes in both HbCO A and rHbCO(αV96W) upon addition of IHP. However, the overall structures of both HbCO A and rHbCO(αV96W) are preserved as manifested by the similarity of their respective $^{15}N-^{1}H$ HSQC spectra in the absence and presence of IHP (Figure 1A,C). Due to the absence of a high-resolution crystal structure of HbCO A complexed with IHP, we have used the same series of HbCO A quaternary structures interpolated between R and R2, which are generated using $\alpha\beta$ dimer structures based on the high-resolution R2 (PDB entry 1BBB) crystal structure for HbCO A, as a basis for fitting the measured RDCs in the presence and absence of IHP, ignoring the small errors brought about by local conformational changes caused by IHP binding. Furthermore, the low-resolution (2.5 Å) R-state crystal structure (PDB entry 1RVW) of the low-oxygen-affinity mutant rHb(αV96W) exhibits a considerably larger root-mean-square deviation (rmsd) between the measured and calculated residual dipolar couplings, when compared with the results obtained using the high-resolution (1.7 Å) 1BBB crystal structure of Hb A to define the geometry of the individual $\alpha\beta$ dimers (Table 3). Therefore, we have used the same 1BBB-based intermediate structures to fit the $^{15}N-^{1}H$ RDCs of the quaternary structure of rHbCO(αV96W). Good agreement has been obtained between the observed and calculated $^{15}N-^{1}H$ RDCs for the best-fit structures of both HbCO A and rHb(αV96W) in the presence of IHP (Figure 2).

The 3.75% polyacrylamide gel provides an alignment frame for our HbCO A sample with the alignment tensor magnitude (D_a) fitted for the optimal quaternary structure and the calculated angle (ϕ) between the principal z-axis of the alignment tensor and the R−R2 dimer rotation axis in very good agreement with those previously determined in bicelles. Thus, it is not surprising that the studies of $^{15}N-^{1}H$ RDCs using stretched gels exhibit an excellent consistency

with the analysis of the $^{15}N-^{1}H$ RDCs measured in bicelles. The optimum quaternary structures, obtained from the minimum in the plots of x_v^2 versus the coordinate x, occur at $x = 0.52 \pm 0.12$ and 0.51 ± 0.13 for the gel and bicelles, respectively, in the absence of IHP. This result validates the choice of the stretched (radially compressed) gel for orienting the hemoglobin molecules, a choice made necessary because the IHP disrupts the bicelle medium (results not shown). Furthermore, the labeled hemoglobin can be recovered relatively easily from the gel, while it cannot be recovered from bicelles. The Pf1 phage orients the Hb tetramers along an axis, which is less favorable for evidencing the quaternary structure change that we are investigating. A small shift (0.07) toward R of the optimal structure has been observed in gels upon addition of IHP. The magnitude of the numbers associated with the IHP binding effect may not seem statistically significant, considering the large fitting error in the results. However, in terms of the averaged quaternary structure, our study shows a clear trend of the structural shift of HbCO A from the R2 toward the R state in the presence of IHP, an allosteric effector, which greatly decreases the oxygen affinity of hemoglobin.

Comparable to the IHP binding effect ($0.52 \rightarrow 0.45$) observed for HbCO A, a nearly identical difference ($0.52 \rightarrow 0.46$) is seen for rHbCO(αV96W) relative to HbCO A, in the absence of IHP. This result indicates that the averaged quaternary structure of rHbCO(αV96W) may be closer to the R structure (i.e., shifted toward the T state) than that of HbCO A, which is consistent with the lower oxygen affinity of this rHb. The corresponding IHP effect on rHbCO-(αV96W) is much larger than on HbCO A. The Δx shift of -0.26 indicates a more noticeable quaternary structure shift from R2 to R in rHbCO(αV96W) upon the binding of IHP, consistent with the finding that the amino acid residues associated with the quaternary structure change in rHbCO-(αV96W) exhibit larger changes in chemical shift and resonance intensity in the presence of IHP than what we have observed in HbCO A.

We have suggested that multiple quaternary structures of hemoglobin, including end-state-ligated conformations and intermediate structures, may coexist under physiological conditions, each of them contributing to the averaged quaternary structure determined as the solution structure (*9*). On the basis of this view of the solution structure, our current study further proposes that, under the modulation of an allosteric effector or site-directed mutagenesis, the contribution of distinct quaternary structures will respond in a fashion such that the population of energetically favorable structures, e.g., the R structure, increases at the expense of unfavorable structures, e.g., the R2 structure. Thus, the solution structure of hemoglobin appears to shift from R2 toward R.

Overall, the trend of the IHP-induced shift of the quaternary structure that we have observed in HbCO A and rHbCO(αV96W) is fundamentally consistent with our previously determined trend in the changes of the P_{50} values under slightly different conditions (*15*), where rHb(αV96W) always exhibits a more pronounced reduction in oxygen affinity (i.e., an increase in P_{50}) upon IHP binding than Hb A does under identical conditions. The oxygen affinity analysis under these experimental conditions at 35 °C also shows a more evident oxygen affinity reduction in rHb(αV96W) than in Hb A (Table 2).

On the basis of structural evidence collected using one-dimensional ^{1}H NMR, ultraviolet difference spectroscopy, ultraviolet circular dichroism spectroscopy, and ultraviolet resonance Raman spectroscopy, Yonetani and co-workers (*13*, *24*) reported that the T and R quaternary states of deoxy-Hb and ligated Hb (oxy- and carbonmonoxy-Hb), respectively, remain unaltered in the presence of various allosteric effectors such as 2,3-BPG, BZF, and IHP. They have proposed that heterotropic effectors are linked only to tertiary structural changes, supposed to be energetically more significant and primarily responsible for modulation of the functions of hemoglobin, rather than to the homotropic ligation-linked T−R quaternary structural transition. Nevertheless, in addition to the IHP-induced tertiary structure change reflected by the chemical shift changes of several amino acid residues in the HSQC spectra, our study of HbCO A and rHbCO(αV96W) based on RDC data clearly indicates the existence of a quaternary structure change from R2 toward R upon the binding of IHP, which is not consistent with the conclusion of Yonetani et al. (*13*). Although neither the one-dimensional ^{1}H NMR study by Yonetani et al. (*13*) nor our multidimensional NMR experiments so far can characterize the tertiary structure change in detail, our observation of IHP-induced quaternary structure change in HbCO A strongly suggests that the conclusion reached by Yonetani and co-workers is questionable and/or at least incomplete. As shown in Figure 2, the best fit of RDCs to a quaternary structure allowed to vary between R and R2 exhibits a quality of fit nearly as good for HbCO A in the presence of IHP (rmsd = 1.41 Hz) as in its absence (rmsd = 1.23 Hz). However, both fits were performed using structures composed of subunits with identical tertiary structures, taken from PDB entry 1BBB, an X-ray structure of HbCO A without IHP. This result suggests that any changes to the tertiary structure induced by IHP binding are relatively minor. The significantly larger quaternary structure change observed in rHbCO(αV96W), when considered together with the more marked decrease in oxygen affinity caused by IHP binding (Table 2), suggests that the quaternary structure change plays an important role in the regulation of the function of hemoglobin by IHP. This does not preclude the possibility that the contribution due to the tertiary structural changes induced by the mutation at position α96 and/or the presence of IHP can alter the oxygen binding properties of this rHb. As mentioned above, an allosteric effect can alter both quaternary and tertiary structures of the Hb molecule, thus altering its ligand affinity. Additional research is needed to ascertain this.

Allosteric Pathway in Hemoglobin. The transition among the three crystal structures of hemoglobin is not fully understood and is controversial; i.e., both $T \rightarrow R2 \rightarrow R$ and $T \rightarrow R \rightarrow R2$ transition pathways have been advocated (*4*, *25*−*29*). A computational analysis carried out by Srinivasan and Rose (*7*) has suggested that the $T \rightarrow R \rightarrow R2$ transition is the more likely allosteric pathway due to the significant geometrical difficulties in the $T \rightarrow R2 \rightarrow R$ transition. The $^{15}N-^{1}H$ RDC analysis, presented here, of hemoglobin based on the HSQC-TROSY method indicates that both site-directed mutagenesis at αV96W and the allosteric effector, IHP, cause a slight shift of the time-averaged quaternary

structure in solution away from R2 and toward R, which is geometrically closer to the deoxy-T structure as proposed by Srinivasan and Rose (*7*) and Mueser et al. (*6*). The effect of IHP on the quaternary structure shift from R2 to R is significantly stronger in rHbCO(αV96W) than in HbCO A. The RDCs collected by using an independent TROSY-based *J*-modulated experiment (*30*) also display a similar trend of the transition induced by IHP in HbCO A and rHbCO-(αV96W) (results not shown). Kim et al. (*15*) also reported that, in their one-dimensional ^{1}H NMR study of rHbCO-(αV96W), the quaternary structure in solution moves to a structure with a deoxy-like $\alpha_1\beta_2$ interface very similar to the T-state structure upon the binding of IHP, especially at a low temperature (10 °C), as evidenced by the appearance of the T structural marker, the exchangeable resonance at 14 ppm, i.e., the intersubunit H-bond between αTyr42 and βAsp99 in the $\alpha_1\beta_2$ subunit interface in the T structure of deoxy-Hb A (*2*, *31*). Our current study supports the suggestion of Srinivasan and Rose (*7*) that the R structure is not only the geometric intermediate but also the thermodynamic intermediate between two distinct populations of hemoglobin, R2 and T.

Very recently, two additional X-ray quaternary structures termed R3 and RR2 have been introduced into the family of ligated Hb A structures by Safo and Abraham (*8*). R3 is believed to be an end state that exhibits a quaternary structure difference from T as large as that between R2 and T, but in a different direction as defined by a rigid-body screw rotation, while RR2 is described as an intermediate conformation between the R and R2 structures. Two new allosteric pathways suggested by Safo and Abraham, T → R → RR2 → R2 and T → R → R3, have further complicated our understanding of Hb allostery. We have applied our RDC method to the structural data on RR2 and R3 and have compared the calculated RDCs for R3 (based on the 1YZI structure) and RR2 (based on the 1MKO structure) with our measured RDCs for HbCO A. In other words, we have fitted our measured RDCs of HbCO A in the absence of IHP to the crystal structures of R (1IRD), RR2 (1MKO), R2 (1BBB), and R3 (1YZI) and tested the correlation between observed RDCs and calculated RDCs (Figure 3). The best correlations are observed for R and R2, where the quality factor *Q* (*32*) values are 14.6 and 15.2%, respectively. A poor correlation ($Q = 17.9\%$) is obtained for RR2, consistent with the lower resolution (2.18 Å) of its crystal structure compared to those of R (1.25 Å) and R2 (1.7 Å), and a much poorer correlation ($Q = 26.4\%$) is seen for R3 (2.07 Å). These results indicate that the actual solution structure is closer to R, RR2, and R2 than to R3 and suggest that the allosteric transition pathway for Hb is more likely the T → R → RR2 → R2 pathway rather than the T → R → R3 pathway.

Although shown by our data not to be in the major allosteric transition pathway, R3 may still represent a quaternary structure relevant to ligated Hb. Safo et al. (*5*, *33*) and Safo and Abraham (*8*) indicate that both R2 and RR2 ligated Hb, whose crystals are usually obtained under low-salt conditions, can be crystallized using high-salt conditions. Thus, there is a question of whether R, RR2, R2, R3, and some other structures intermediate between R and R2 (*6*, *29*, *33*, *34*) represent different physiological states of ligated Hb or are just crystallized in response to subtle

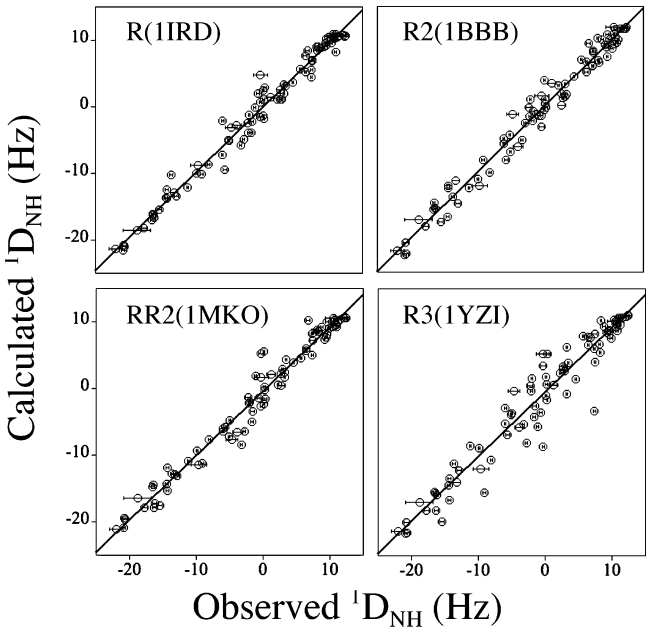

FIGURE 3: Correlation between observed and calculated RDCs, based on the crystal structures R (1IRD), R2 (1BBB), RR2 (1MKO), and R3 (1YZI). The quality factors (*Q*) are 14.6, 15.2, 17.9, and 26.4%, respectively. Errors calculated as described for the observed RDCs are shown.

changes in experimental conditions. To address this question, Safo and Abraham (*8*) raise the possibility that R, RR2, R2, R3, and other potential ligated forms may have varied affinities for oxygen. Several reports (*35*−*38*) have supported this concept and shown that Hb behaves like a multistate system. An important question that needs to be addressed is how much these R-type structures exist in solution as individual structures and exhibit unique functional properties or whether they interconvert among themselves and on what time scale. According to our NMR results, the solution structure of Hb A and rHb(αV96W) in the CO form is a dynamic ensemble of the R and R2 crystal structures, and the alteration in the functional properties of hemoglobins by IHP is most likely due to changes in both quaternary and tertiary structures of the protein molecule. There is yet no direct information that deoxy-Hbs exhibit multiple T types of structures in crystalline and solution states. The available evidence strongly supports the concept that ligated hemoglobin is a multi-physiological-state system. Hemoglobin is a very flexible molecule that can respond to changes in its environment. For example, the oxygen affinity of Hb can either be diminished in the presence of allostertic effectors such as 2,3-bisphosphoglycerate and IHP (*1*) or increased in the presence of antisickling drugs such as furanic compounds (*5*). The dynamic picture of hemoglobin is consistent with the emerging view of allostery (*39*−*40*) as a change in the population distribution of an ensemble of structures, rather than the equilibrium of only two discrete conformations, upon ligand binding. Complementary information is provided by X-ray crystallography, which reveals a "snapshot" of the most favorable structure crystallized under given conditions, and NMR, which provides dynamically averaged properties. Ensemble-based molecular modeling studies (*41*, *42*) point to the importance of a wide range of states, including those only minutely populated, to the propagation of binding energy between distant sites. Thus,

a full understanding of the molecular basis of allostery will require the investigation of transiently visited (i.e., low-population) high-energy states of proteins; very useful in this regard will be the technique of relaxation−dispersion NMR, which can characterize states whose population is too low to be observed directly (*43*). In the context of these recent results, the classic two-state/two-structure T/R allosteric model advocated by Perutz (*2*) has to be revised to account for the structural, dynamic, and functional properties of proteins including hemoglobin.

ACKNOWLEDGMENT

We thank Dr. Nico Tjandra and Dr. Cheryl Hawkins for giving us very helpful suggestions for the preparation of the polyacrylamide gel and Dr. E. Ann Pratt for helpful discussions about our manuscript.

REFERENCES

1. Dickerson, R. E., and Geis, I. (1983) *Hemoglobin: Structure, Function, Evolution and Pathology*, Benjamin Cummings, Menlo Park, CA.
2. Perutz, M. F. (1970) Stereochemistry of cooperative effects in haemoglobin, *Nature 228*, 726−39.
3. Perutz, M. F. (1968) Preparation of Hb Crystals, *J. Cryst. Growth 2*, 54−6.
4. Silva, M. M., Rogers, P. H., and Arnone, A. (1992) A third quaternary structure of human hemoglobin A at 1.7-Å resolution, *J. Biol. Chem. 267*, 17248−56.
5. Safo, M. K., Abdulmalik, O., Danso-Danquah, R., Burnett, J. C., Nokuri, S., Joshi, G. S., Musayev, F. N., Asakura, T., and Abraham, D. J. (2004) Structural basis for the potent antisickling effect of a novel class of five-membered heterocyclic aldehydic compounds, *J. Med. Chem. 47*, 4665−76.
6. Mueser, T. C., Rogers, P. H., and Arnone, A. (2000) Interface sliding as illustrated by the multiple quaternary structures of liganded hemoglobin, *Biochemistry 39*, 15353−64.
7. Srinivasan, R., and Rose, G. D. (1994) The T-to-R transformation in hemoglobin: A reevaluation, *Proc. Natl. Acad. Sci. U.S.A. 91*, 11113−7.
8. Safo, M. K., and Abraham, D. J. (2005) The enigma of the liganded hemoglobin end state: A novel quaternary structure of human carbonmonoxy hemoglobin, *Biochemistry 44*, 8347−59.
9. Lukin, J. A., Kontaxis, G., Simplaceanu, V., Yuan, Y., Bax, A., and Ho, C. (2003) Quaternary structure of hemoglobin in solution, *Proc. Natl. Acad. Sci. U.S.A. 100*, 517−20.
10. Arnone, A. (1972) X-ray diffraction study of binding of 2,3-diphosphoglycerate to human deoxyhaemoglobin, *Nature 237*, 146−9.
11. Arnone, A., and Perutz, M. F. (1974) Structure of inositol hexaphosphate−human deoxyhaemoglobin complex, *Nature 249*, 34−6.
12. Kavanaugh, J. S., Rogers, P. H., and Arnone, A. (2005) Crystallographic evidence for a new ensemble of ligand-induced allosteric transitions in hemoglobin: The T-to-T(high) quaternary transitions, *Biochemistry 44*, 6101−21.
13. Yonetani, T., Park, S. I., Tsuneshige, A., Imai, K., and Kanaori, K. (2002) Global allostery model of hemoglobin. Modulation of O_2 affinity, cooperativity, and Bohr effect by heterotropic allosteric effectors, *J. Biol. Chem. 277*, 34508−20.
14. Marden, M. C., Kister, J., Bohn, B., and Poyart, C. (1988) T-State hemoglobin with four ligands bound, *Biochemistry 27*, 1659−64.
15. Kim, H. W., Shen, T. J., Sun, D. P., Ho, N. T., Madrid, M., and Ho, C. (1995) A novel low oxygen affinity recombinant hemoglobin (α96Val→Trp): Switching quaternary structure without changing the ligation state, *J. Mol. Biol. 248*, 867−82.
16. Mozzarelli, A., Rivetti, C., Rossi, G. L., Eaton, W. A., and Henry, E. R. (1997) Allosteric effectors do not alter the oxygen affinity of hemoglobin crystals, *Protein Sci. 6*, 484−9.
17. Tsai, C. H., Shen, T. J., Ho, N. T., and Ho, C. (1999) Effects of substitutions of lysine and aspartic acid for asparagine at β108 and of tryptophan for valine at α96 on the structural and functional properties of human normal adult hemoglobin: Roles of $\alpha_1\beta_1$ and $\alpha_1\beta_2$ subunit interfaces in the cooperative oxygenation process, *Biochemistry 38*, 8751−61.
18. Fang, T. Y., Simplaceanu, V., Tsai, C. H., Ho, N. T., and Ho, C. (2000) An additional H-bond in the $\alpha_1\beta_2$ interface as the structural basis for the low oxygen affinity and high cooperativity of a novel recombinant hemoglobin (βL105W), *Biochemistry 39*, 13708−18.
19. Puius, Y. A., Zou, M., Ho, N. T., Ho, C., and Almo, S. C. (1998) Novel water-mediated hydrogen bonds as the structural basis for the low oxygen affinity of the blood substitute candidate rHb-(α96Val→Trp), *Biochemistry 37*, 9258−65.
20. Simplaceanu, V., Lukin, J. A., Fang, T. Y., Zou, M., Ho, N. T., and Ho, C. (2000) Chain-selective isotopic labeling for NMR studies of large multimeric proteins: Application to hemoglobin, *Biophys. J. 79*, 1146−54.
21. Chou, J. J., Gaemers, S., Howder, B., Louis, J. M., and Bax, A. (2001) A simple apparatus for generating stretched polyacrylamide gels, yielding uniform alignment of proteins and detergent micelles, *J. Biomol. NMR 21*, 377−82.
22. Lukin, J. A., Kontaxis, G., Simplaceanu, V., Yuan, Y., Bax, A., and Ho, C. (2004) Backbone resonance assignments of human adult hemoglobin in the carbonmonoxy form, *J. Biomol. NMR 28*, 203−4.
23. Tjandra, N., and Bax, A. (1997) Direct measurement of distances and angles in biomolecules by NMR in a dilute liquid crystalline medium, *Science 278*, 1111−4.
24. Nagatomo, S., Nagai, M., Mizutani, Y., Yonetani, T., and Kitagawa, T. (2005) Quaternary structures of intermediately ligated human hemoglobin a and influences from strong allosteric effectors: Resonance Raman investigation, *Biophys. J. 89*, 1203−13.
25. Doyle, M. L., Lew, G., Turner, G. J., Rucknagel, D., and Ackers, G. K. (1992) Regulation of oxygen affinity by quaternary enhancement: Does hemoglobin Ypsilanti represent an allosteric intermediate, *Proteins: Struct., Funct., Genet. 14*, 351−62.
26. Smith, F. R., Lattman, E. E., and Carter, C. W., Jr. (1991) The mutation β99 Asp-Tyr stabilizes Y: A new, composite quaternary state of human hemoglobin, *Proteins 10*, 81−91.
27. Smith, F. R., and Simmons, K. C. (1994) Cyanomet human hemoglobin crystallized under physiological conditions exhibits the Y quaternary structure, *Proteins 18*, 295−300.
28. Janin, J., and Wodak, S. J. (1993) The quaternary structure of carbonmonoxy hemoglobin Ypsilanti, *Proteins 15*, 1−4.
29. Schumacher, M. A., Zheleznova, E. E., Poundstone, K. S., Kluger, R., Jones, R. T., and Brennan, R. G. (1997) Allosteric intermediates indicate R2 is the liganded hemoglobin end state, *Proc. Natl. Acad. Sci. U.S.A. 94*, 7841−4.
30. Luy, B., and Marino, J. P. (2003) JE-TROSY: Combined J- and TROSY-spectroscopy for the measurement of one-bond couplings in macromolecules, *J. Magn. Reson. 163*, 92−8.
31. Fung, L. W., and Ho, C. (1975) A proton nuclear magnetic resonance study of the quaternary structure of human homoglobins in water, *Biochemistry 14*, 2526−35.
32. Ottiger, M., Delaglio, F., and Bax, A. (1998) Measurement of J and dipolar couplings from simplified two-dimensional NMR spectra, *J. Magn. Reson. 131*, 373−8.
33. Safo, M. K., and Abraham, D. J. (2001) The X-ray structure determination of bovine carbonmonoxy hemoglobin at 2.1 Å resoultion and its relationship to the quaternary structures of other hemoglobin crystal froms, *Protein Sci. 10*, 1091−9.
34. Sutherland-Smith, A. J., Baker, H. M., Hofmann, O. M., Brittain, T., and Baker, E. N. (1998) Crystal structure of a human embryonic haemoglobin: The carbonmonoxy form of gower II ($\alpha_2\epsilon_2$) haemoglobin at 2.9 Å resolution, *J. Mol. Biol. 280*, 475−84.
35. Perrella, M., Benazzi, L., Shea, M. A., and Ackers, G. K. (1990) Subunit hybridization studies of partially ligated cyanomethemoglobins using a cryogenic method. Evidence for three allosteric states, *Biophys. Chem. 35*, 97−103.
36. Bucci, E., Fronticelli, C., and Gryczynski, Z. (1991) Discontinuous release of heat at successive steps of oxygenation in human and bovine hemoglobin at pH 9.0, *Biochemistry 30*, 3195−9.
37. Jayaraman, V., and Spiro, T. G. (1995) Structure of a third cooperativity state of hemoglobin: Ultraviolet resonance Raman spectroscopy of cyanomethemoglobin ligation microstates, *Biochemistry 34*, 4511−5.
38. Bucci, E., Razynska, A., Kwansa, H., Gryczynski, Z., Collins, J. H., Fronticelli, C., Unger, R., Braxenthaler, M., Moult, J., Ji, X.,

and Gilliland, G. (1996) Positive and negative cooperativities at subsequent steps of oxygenation regulate the allosteric behavior of multistate sebacylhemoglobin, *Biochemistry 35*, 3418−25.
39. Kern, D., and Zuiderweg, E. R. P. (2003) The role of dynamics in allosteric regulation, *Curr. Opin. Struct. Biol. 13*, 748−57.
40. Gunasekaran, K., Ma, B., and Nussinov, R. (2004) Is allostery an intrinsic property of all dynamic proteins? *Proteins: Struct., Funct., Bioinf. 57*, 433−43.
41. Pan, H., Lee, C., and Hilser, V. J. (2000) Binding sites in *Escherichia coli* dihydrofolate reductace communicate by modulating the conformational ensemble, *Proc. Natl. Acad. Sci. U.S.A. 97*, 12020−5.
42. Liu, T., Whitten, S. T., and Hilser, V. J. (2006) Ensemble-based signatures of energy propagation in proteins: A new view of an old phenomenon, *Proteins: Struct., Funct., Bioinf. 62*, 728−38.
43. Korzhnev, D. M., Salvatella, X., Vendruscolo, M., Di Nardo, A. A., Davidson, A. R., Dobson, C. M., and Kay, L. E. (2004) Low-populated folding intermediates of FYN SH3 characterized by relaxation dispersion NMR, *Nature 430*, 586−90.
44. Bax, A., Kontaxis, G., and Tjandra, N. (2001) Dipolar couplings in macromolecular structure determination, *Methods Enzymol. 339*, 127−74.

BI052424H